Theoretical Computation of the Isothermal Flow Through the Reverse Screw Element of a Twin Screw Extrusion Cooker

J. Tayeb, B. Vergnes, G. Della. Valle

Reprinted from J. Food Sci.
53(2): 616–625

Theoretical Computation of the Isothermal Flow Through the Reverse Screw Element of a Twin Screw Extrusion Cooker

J. TAYEB, B. VERGNES, and G. DELLA VALLE

ABSTRACT

A mathematical model of the flow of molten starch through the reverse screw element of a twin screw extrusion-cooker was proposed. The assumptions included isothermicity, Newtonian flow in each part of the reverse screw element and quasi-steady geometry. The theoretical approach is based on solving Stokes equations in the direct screw element and then on writing flow rate conservation in each part of the reverse screw element. The various flow rates, the pressure drop and the residence time distribution through the reverse screw element were computed for a CLEXTAL **BC 45** twin screw extruder under different operating and geometrical conditions; good agreement was found when comparing these results with previous experimental work. The pressure drop through the reverse screw element was low (0.5–1.0 MPa); the flow rates in the different channels of the reverse screw element were important compared to the total feed rate of the extruder (two to three times larger) which might explain the broadening of the residence time distribution in the reverse screw element.

INTRODUCTION

Extrusion-cooking is an efficient and versatile food processing technology which is finding an increased use in industry to fabricate a wide variety of products including snack food, flat breads, breakfast cereals, pet food and texturized proteins (Harper, 1981; Linko et al., 1981). These products are made on empirical basis, as food extruder modeling is still in development.

Modeling of the flow in an extruder depends principally on the type of extruder: single screw, counter-rotating or co-rotating twin screw. Simplest systems are single screw and counter-rotating twin screw. In these machines, the geometry may be approximated to a continuous channel (single screw food extruders: Harmann and Harper, 1974; Bruin et al., 1978; Pisipati and Fricke, 1980) or to closed C-shaped chambers (counter-rotating twin screw: Janssen, 1978). In the field of co-rotating twin screw extruders, relatively few investigations have been documented (Masheri and Wyman, 1980; Denson and Hwang, 1980; Booy, 1980; Martelli, 1983; Yacu, 1985).

In co-rotating twin screw extruders, screw configuration often includes kneading paddles or reverse screw elements. The reverse screw elements (RSE) are characterized by a reverse flight pushing the product backward; some axial openings called "axial slots" are grooved in the screw flight, allowing the product to go forward through the RSE. It is well known that the RSE increases the filling rate of the screw and that the transformation of the product occurs mainly in this section (Colonna et al., 1983). Physical measurements of pressure and product temperature have also shown the importance of the reverse screw element (Fletcher et al., 1984; Della Valle et al., 1987).

Authors Tayeb and Della Valle are with Institut National de la Recherche Agronomique, Laboratoire de Biochimie et Technologie des Glucides, Rue de la Géraudière, 44072 Nantes Cédex 03-France. Author Vergnes is with the Centre de Mise en Forme des Matériaux, UA 852, Ecole Nationale Supérieure des Mines de Paris, Sophia-Antipolis, 06560 Valbonne-France.

The aim of the present work was to model the flow through the reverse screw element to better understand the effects of this element on pressure drop, flow rate and residence time distribution. Maize starch was chosen as a model product; it is the basis of many commerical, extrusion-cooked foods, and its rheology has been previously studied (Vergnes et al., 1985; Vergnes and Villemaire, 1987).

The study presented was part of a work aimed to model the whole twin screw extruder by a step by step analysis of the various functional zones: transport, pressure build up, reverse screw element and die. The description of flows through the extruder should be used to calculate thermomechanical history of the product (temperature field, pressure field, shearing field, time) in order to predict its transformation, as did Vergnes et al. (1987) in an apparatus simulating the extruder. The interest of such an approach is double: the extruder manufacturer can enhance the geometry and scale up the machine properly; the product manufacturer can predict which are the most efficient control variables and how to choose the working point of the machine to obtain a given product.

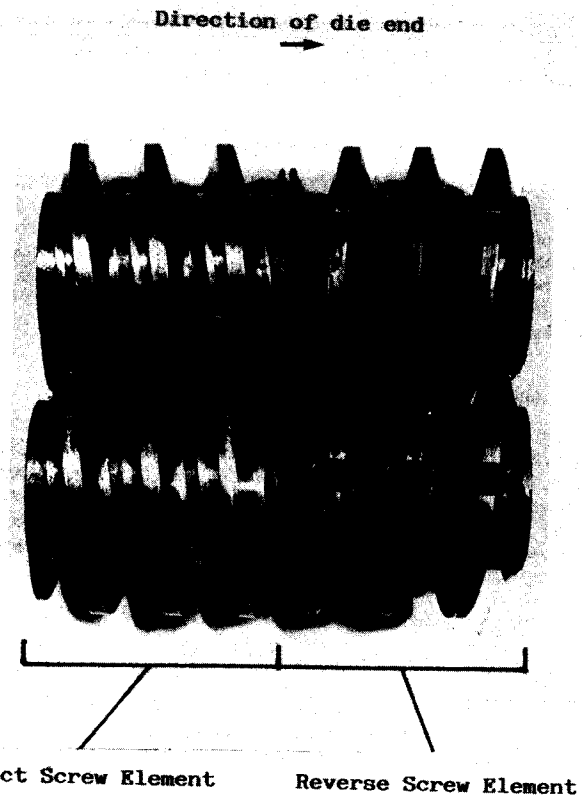

Fig. 1—Section of the screw, closer to the die, showing a direct screw element and a reverse screw element with parallel axial slots (CLEXTRAL BC 45).

Table 1—Coefficients of the power law $\eta = K\dot{\gamma}^{m-1}$[a]

Added water (%)	0		10		20		30	
Water content (%)	13		21		28		33	
Temperature (°C)	150	170	150	170	150	170	150	170
Consistency K (Pa.s^m)	23740	14450	12770	7770	6870	4180	3700	2250
Pseudo-plasticity index m	0.29	0.33	0.37	0.42	0.44	0.51	0.52	0.59

[a] Vergnes et al. (1985)

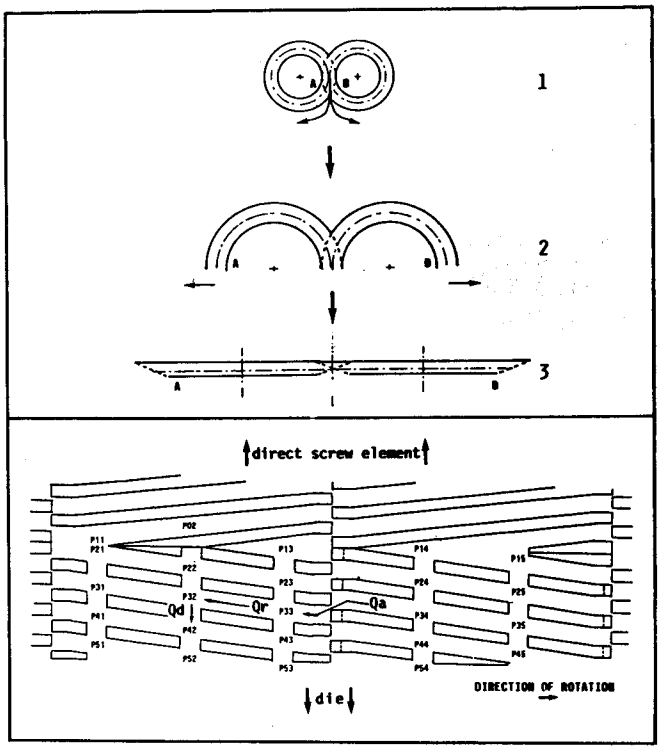

Fig. 2—"Unrolling" of the RSE *geometry and resulting* **RSE** *schemes (axial section and overhead view).*

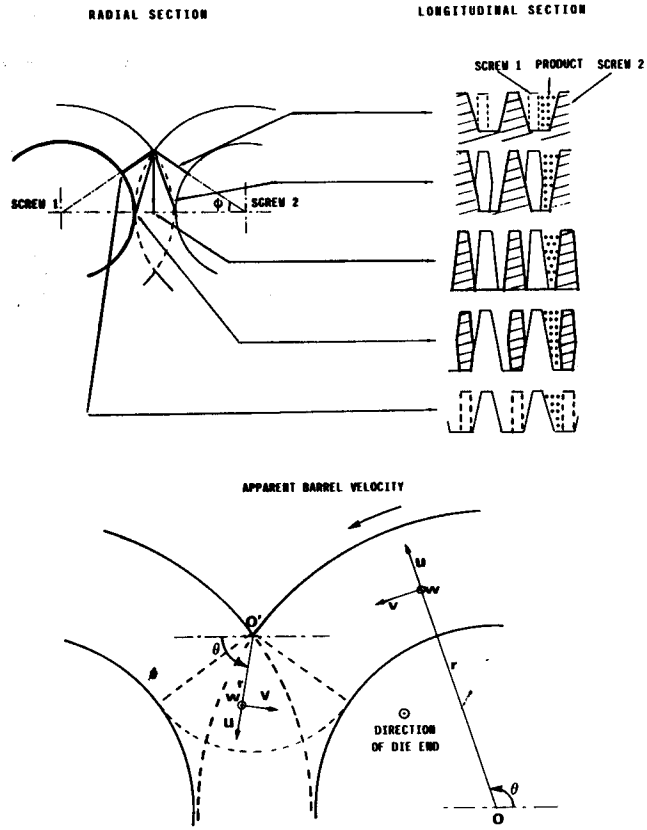

Fig. 3—Coordinate Systems used in the flow description and local geometry of the intermeshing zone (cross sections at different positions).

THEORETICAL APPROACH

THE THEORETICAL STUDY was divided into three parts: (1) a geometrical description to determine the parameters necessary for the computation and to define the kinematic phenomena; (2) the solution of Stokes equations in the direct screw element to describe the relations between pressure and flow rate in the regular channel and in the intermeshing zone; and (3) finally, to obtain the local flows in the RSE by writing flow rate conservation.

Geometrical description

The geometry of the RSE depends on the characteristics of the screw and the axial slots. The screw is entirely defined by five parameters (Booy, 1978): the external radius (Re), the distance between the two screw shafts (Cl), the pitch of the screw (Bs), the flight width at the top (Fe) and at the bottom (Fi) of the channel. From these dimensions, the screw channel depth (h) and the intermeshing angle (ψ) may be obtained:

$$h \approx 2\,Re - Cl$$

$$\Psi = \cos^{-1}(Cl/2\,Re)$$

The axial slots may be drilled either parallel or helicoidal to the shafts (Fig. 1). Only the case with axial slots parallel to the shaft was treated; a similar approach could be developed for the other case. The axial slots are defined by their width (la) and their number per turn of screw (Na). For better understanding, a plane representation of the RSE geometry was used. Figure 2 illustrates the unrolling process; however, the equations of flow were written in the circular geometry, with a cylindrical coordinate system (Fig. 3). The cross section of the channel has a trapezoidal shape, but for simplification in computation, it was assumed to have an equivalent rectangular shape (width, lv). The intermeshing zone between the two screws needs to be carefully described (Fig 3). This zone was approximated by a portion of circular channel of reduced width; its cross section is nearly trapezoidal and is described by an equivalent rectangle (width, lw).

Like in single screw extruder modeling, the equations of flow were locally written assuming that the screws were stationary with the barrel slipping over it. In this case (Wyman, 1975; Booy, 1978), the barrel speed above each screw is Ω Re (Ω: screw speed). The kinematics of the intermeshing zone is complex; it may be shown that the principal motion is the displacement of the flank of one screw relative to the flank of the other screw, at a speed of ClΩ (Tayeb, 1986).

In the RSE, the rotation of the screws makes the geometry vary periodically; no flow is possible through an axial slot which is in the intermeshing zone facing the non opened flank of the other screw. A systematic study of the different screw positions (Fig. 4) showed that the most frequent configurations were those with three open slots on one screw and two on the other one. One of these configurations was principally studied, but the results were compared with those from other configurations to verify that a "quasi-steady" approach was valid.

Equations of flow in the direct screw element

Hypothesis and boundary conditions. In the direct screw element, the flow equations were written assuming the following hypothesis:

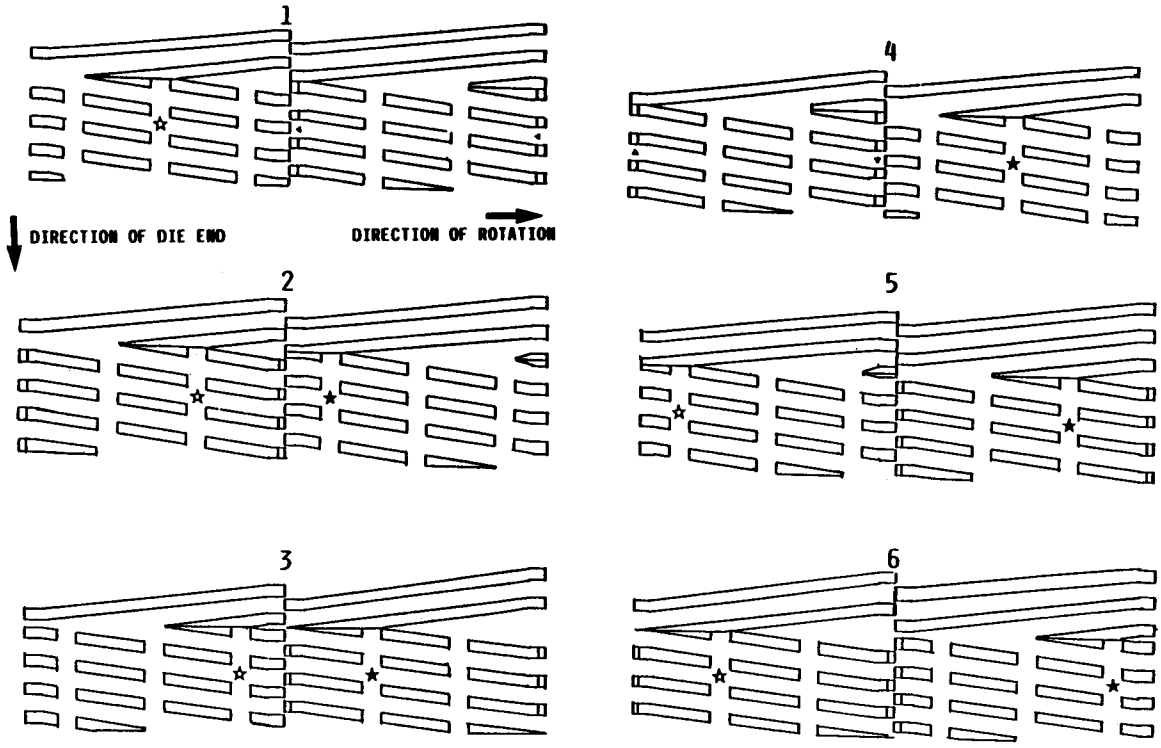

Fig. 4—Different RSE *Configurations observed during the screw rotation(☆ and ★ show the motion of given axial slots).*

the flow was steady, fully developed and isothermal; the viscosity was constant (Newtonian behavior); the slip at the screw and at the barrel walls was negligible; body and inertia forces were negligible.

The following assumptions were made about the velocity field: $u(r,\theta,z)=O$ (no radial velocity); $v(r,\theta,z)=v(r)$ (down-channel velocity was a function of r only); $w(r,\theta,z)=w(r)$ (cross-channel velocity was a function of r only). Moreover, it was assumed that over the integration range the axial and tangential pressure gradients, $\partial P/\partial\theta$ and $\partial P/\partial z$, were constants.

Boundary conditions corresponding to the slipping barrel assumptions (φ being the pitch angle of the screw) were $v(Re) = Ve = \Omega\, Re\cos(\varphi)$ and $w(Re) = We = \Omega\, Re\sin(\varphi)$.

Solution of the Stokes equations. With the above hypothesis, Stokes equations on v(r) and w(r) were written as follows:

$$\frac{1}{\eta}\frac{\partial P}{\partial \theta} = r\frac{\partial}{\partial r}\left(\frac{1}{r}\frac{\partial}{\partial r}(rv)\right) \tag{1}$$

$$\frac{1}{\eta}\frac{\partial P}{\partial z} = \frac{1}{r}\frac{\partial}{\partial r}\left(r\frac{\partial w}{\partial r}\right) \tag{2}$$

$\partial P/\partial\theta$ and $\partial P/\partial z$ being constant, Eq. (1) and (2) were simplified as:

$$\frac{\partial}{\partial r}\left(\frac{1}{r}\frac{\partial}{\partial r}(rv)\right) = \frac{\alpha}{r} \tag{3}$$

$$\frac{\partial}{\partial r}\left(r\frac{\partial w}{\partial r}\right) = \beta r \tag{4}$$

with $\alpha = \Delta P/(\eta\Delta\theta)$ and $\beta = \Delta P/(\eta\Delta z)$.

The integration of Eq. (3) and (4) with the boundary conditions $v(Re) = Ve$ and $w(Re) = We$ gave the expression of the down-channel and the cross-channel velocities:

$$v(r) = \frac{1}{2\eta}\frac{\Delta P}{\Delta\theta}\left[r\left(\frac{Re^2\ln(r/Re) - Ri^2\ln(r/Ri)}{Re^2 - Ri^2}\right) + \frac{1}{r}\frac{Re^2\,Ri^2}{Re^2 - Ri^2}\ln\left(\frac{Re}{Ri}\right)\right] + Ve\frac{Re}{r}\left(\frac{r^2 - Ri^2}{Re^2 - Ri^2}\right) \tag{5}$$

$$w(r) = \frac{1}{4\eta}\frac{\Delta P}{\Delta z}\left[r^2 - \left(\frac{Re^2\ln(r/Ri) - Ri^2\ln(r/Re)}{\ln(Re/Ri)}\right)\right] + We\frac{\ln(r/Ri)}{\ln(Re/Ri)} \tag{6}$$

Integrating the velocities over the channel depth lead to the expressions of the flow rates:

$$\frac{Qv}{Iv} = -Fp_v\frac{1}{8\eta}\frac{\Delta P}{\Delta\theta}(Re^2 - Ri^2)\left[1 - \left(\frac{2\,Re\,Ri}{Re^2 - Ri^2}\ln\left(\frac{Re}{Ri}\right)\right)^2\right] + Fd_v\frac{1}{2}Ve\,Re\left[1 - \left(\frac{Ri^2}{Re^2 - Ri^2}\ln\left(\frac{Re}{Ri}\right)^2\right)\right] \tag{7}$$

$$\frac{Qw}{Iw} = -Fp_w\frac{1}{4\eta}\frac{\Delta P}{\Delta z}\left[\frac{2}{3}(Re^3 - Ri^3) - \left(\frac{Re^3 + Ri^3 - Ri\,Re^2 + Ri^2\,Re}{\ln(Re/Ri)}\right)\right] + Fd_w\,We\,Re\left[1 - \left(\frac{1 - Ri/Re}{\ln(Re/Ri)}\right)\right] \tag{8}$$

These equations have the classical form of the sum of a drag flow and a pressure flow. Fd and Fp, the respective correction shape factors for the drag flow and the pressure flow, depend on the depth/width ratio of the channel (Rauwendaal, 1986).

In the direct flight screw element, the down-channel flow rate is known (feed rate of the extruder) and the cross-channel flow rate is equal to zero (assuming that the different leakage flows are negligible). Then, Eq. (7) and (8) permit the definition of the pressure gradients $\Delta P/\Delta\theta$ and $\Delta P/\Delta z$, and the complete determination of the velocity fields v(r) and w(r).

Flow field in the reverse screw element

In a longitudinally split barrel of a twin-screw extruder, it has been observed that the reverse screw element was filled with molten material (Colonna et al., 1983). So, in this element, the preceding equations describing a continuous fluid were used.

Three kinds of flows were identified in the RSE: direct flow through

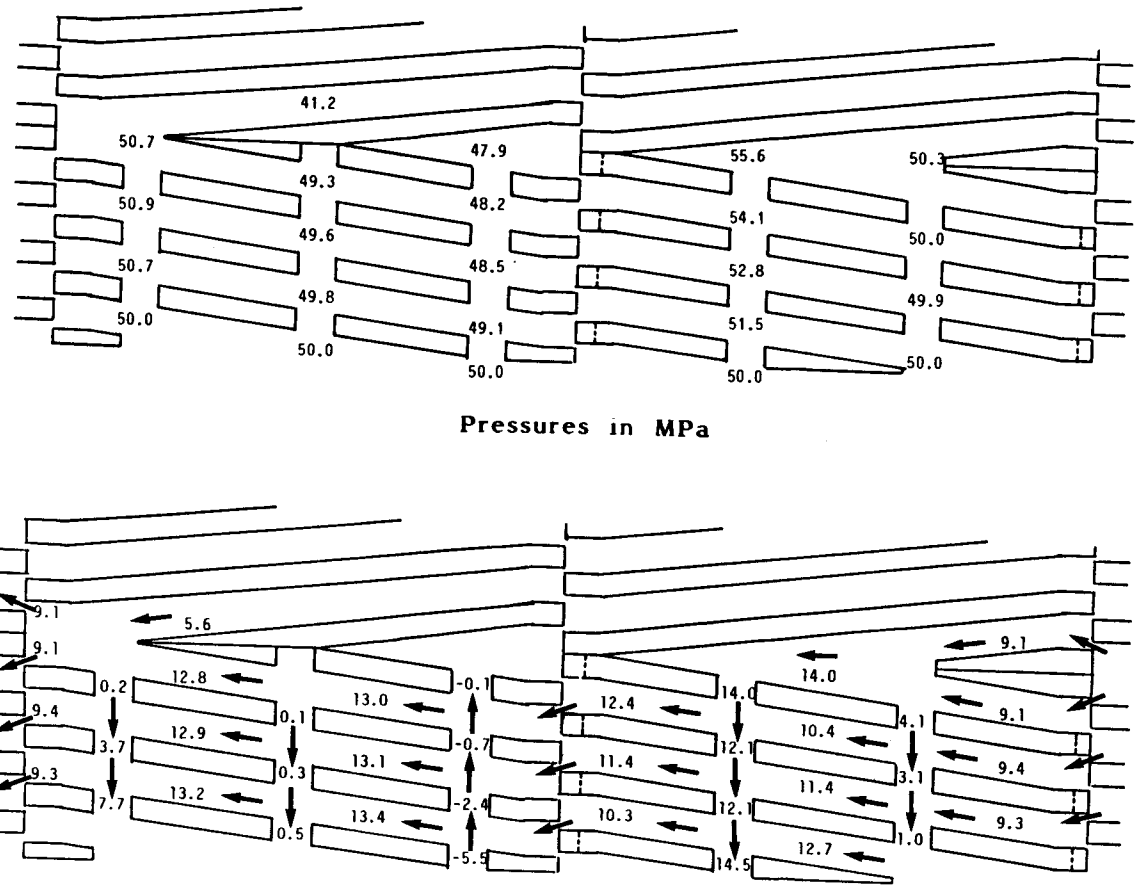

Fig. 5—Computed pressure and flow rate distributions in the standard operating conditions (screw speed 200 =rpm; feed rate = 30 kg/hr).

the axial slot (Qd), reverse flow along the regular backwarding channels (Qr) and reverse flow through the intermeshing zone between the two screws (Qa) (Fig. 2). All the other secondary leakage flows were not taken into account in this first approach. Using the same assumptions as in the direct screw element, each kind of flow was expressed as a sum of a drag flow and a pressure flow:

$$Qr = A + B\,\Delta Pr \quad (9)$$

$$Qd = C + D\,\Delta Pd \quad (10)$$

$$Qa = E + F\,\Delta Pa \quad (11)$$

where A, B, C, D, E, F are different coefficients derived from Eq. (7) and (8) (their expressions are given in appendix) depending on the local geometry, product viscosity and screw rotation speed; ΔPr, ΔPd, ΔPa are the local pressure gradients.

Considering the plane representation of the flow field (Fig. 2), local nodes were defined (numbered by indices i and j) at the intersections of the axial slots and screw channels. The index i (from 1 to 5) is related to the flight number, growing from the first flight of the RSE to the die; in a wider sense, i = O stands for the end of the direct screw element. For a given flight number, the index j (from 1 to 5, increasing in the direction of rotation) corresponds to each axial slot. So P(O,2) was the entrance pressure and P(5,j) the pressure at the die.

At each node, a flow rate conservation equation was written. The sum of the flow rates arriving at and leaving from the node is equal to zero. For instance, at the node (3,2), we had:

$$Qd(2,2) + Qr(3,3) = Qd(3,2) + Qr(3,2) \quad (12)$$

Substituting Eq. (9) and (10) in Eq. (12) leads to:

$$C + D\,[P(2,2) - P(3,2)] + A + B\,[P(3,3) - P(3,2)] = C + D\,[P(3,2) - P(4,2)] + A + B\,[P(3,2) - P(3,1)] \quad (13)$$

or

$$D\,P(2,2) + B\,P(3,1) - 2\,(B+D)\,P(3,2) + B\,P(3,3) + D\,P(4,2) = 0 \quad (14)$$

So a linear relation was obtained between the node pressure (which was P(3,2,) in this instance) and the pressures of the adjacent nodes.

Writing a similar equation for each node of the RSE led to a set of linear equations with the pressures as unknowns. Boundary conditions were defined taking into account the geometry of the transition zone between the direct screw element and the RSE (for instance, no flow exists between node (1,4) and (1,3)). The pressures at the end of the RSE and at the end of the direct screw element (entrance pressure) were assumed to be known.

The resolution of the linear system with the preceding boundary conditions provided the pressures at each node of the mesh. The different flow rates were then computed from Eq. (9) to (11).

RESULTS FROM THEORETICAL MODEL

THE THEORETICAL MODEL admits, as parameters, the geometrical characteristics of the machine (dimensions of the screw, diameter of the die), the operating conditions (screw rotation speed, total feed rate) and the characteristics of the machine (dimensions of the screw, diameter of the die), the operating conditions (screw rotation speed, total feed rate) and the characteristics of the products (viscosity, thermal properties). To check the model, theoretical results have been computed for a CLEXTRAL BC 45 extruder and maize starch for standard operating conditions. In the next part of this paper, these results are compared to previously published experimental data (Mosso et al., 1982; Della Valle et al., 1987).

Geometrical and operating data

The data used in the computation refer to a CLEXTRAL BC 45 twin screw extruder. The reverse screw element was

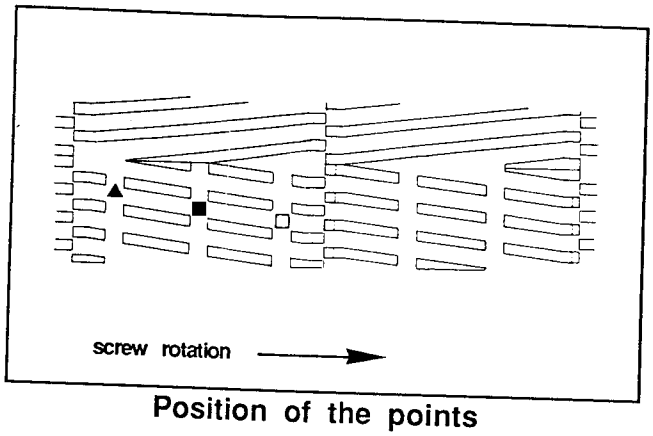

Fig. 6—Evolution of the computed pressure drop and flow rate at given nodes with the screw rotation (Fig. 4).

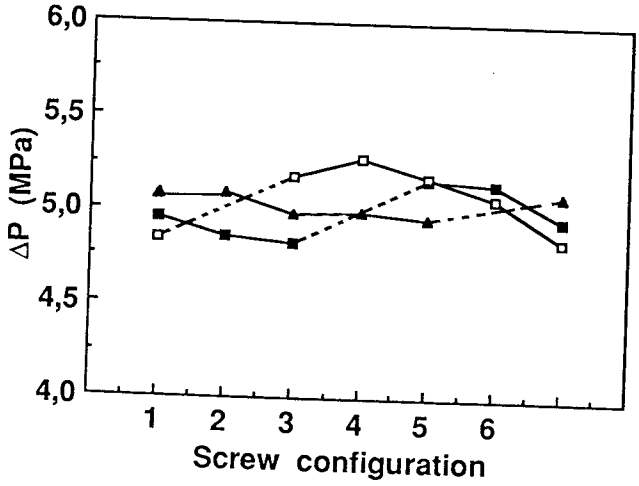

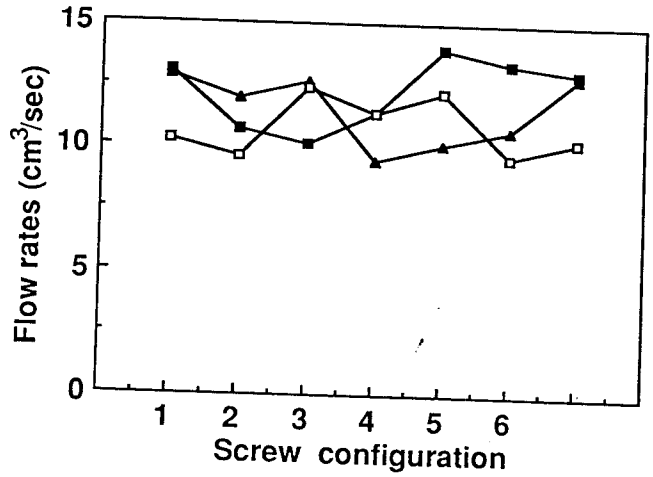

located just before the die; the main geometrical dimensions of the screw and of the RSE were: shaft to shaft distance (Cl), 45 mm; external radius of the screw (Re), 28 mm; pitch of the screw (Bs), 15 mm; flight width at the top (Fe), 3 mm; flight width at the bottom (Fi), 9 mm; number of axial slots per turn (Na), 3; width of the axial slots (Wa), 10 mm.

The rheology of the maize starch has been studied previously (Vergnes et al., 1985; Vergnes and Villemaire, 1987). The numerical value of the Newtonian equivalent viscosity η was computed in each section of the RSE using a power law model, the shear rate being geometrically estimated from screw rotation speed and geometry, which was about 50 sec^{-1} in the channel and 190 sec^{-1} in the intermeshing zone at a screw speed of 200 rpm. The coefficients of the power law estimated at various temperatures and added water are given in Table 1. The computations were made for a product temperature of 150° and 10% added water, in which case K= 12770 and m-1 = −0.63.

The set of operating conditions defined as "standard" are: screw rotation speed =200 rpm, feed rate =30 kg/hr or 5.6 cm^3/sec. First, results obtained in these conditions were examined, then the influence of operating variables was studied.

Computed results at standard operating conditions

The results for the standard operating conditions are shown in Fig. 5. The pressure in the RSE varied between 4.5 and 5.5 MPa for a die pressure of 5.0 MPa. The R- and A-type flow rates were quite centered at about 12 cm^3/sec and 10 cm^3/sec, respectively, but the repartition of the D-type flow rates was broad (between -5 + 14 cm^3/sec), due to the existence of secondary flows.

Comparisons of the computed results obtained in the different geometries generated by the screw rotation (Fig. 4) showed that, at a given node (Fig. 6), pressure and flow rate varied quite smoothly (Fig. 6: ±0.15 MPa for pressures; ±2 cm^3/sec for R-and A-type flow rates) with the screw rotation; so the quasi-steady method used for the analysis may be considered as valid.

Computed influence of operating conditions and geometry

It is not easy to summarize the pressure and flow rate fields in the RSE. The pressure drop was characterized by two values. The first one was the difference between the entrance pressure and the pressure at the die (ΔPe = P(0,2)-P(5,i)), and the second one was the difference between the maximum pressure in the RSE and the pressure at the die (ΔPmax = P(1,4 –P(5,i)). The flow rate field was characterized by the average value of each kind of flow, complemented by the minimum and maximum values for the D-type flow rate, whose repartition was quite broad.

The influences of screw rotation speed and of total feed rate of the extruder are shown in Fig. 7 and 8. ΔPmax increased (+ 0.25 MPa) mainly when screw speed increased (100 to 250 rpm); ΔPe decreased (–1.0 MPa) with screw speed (100 to 250 rpm) and increased (+1.2MPa) with feed rate (2.8 to 11.1 cm^3/sec = 15 to 60 kg/hr). Flow rates increased approx-

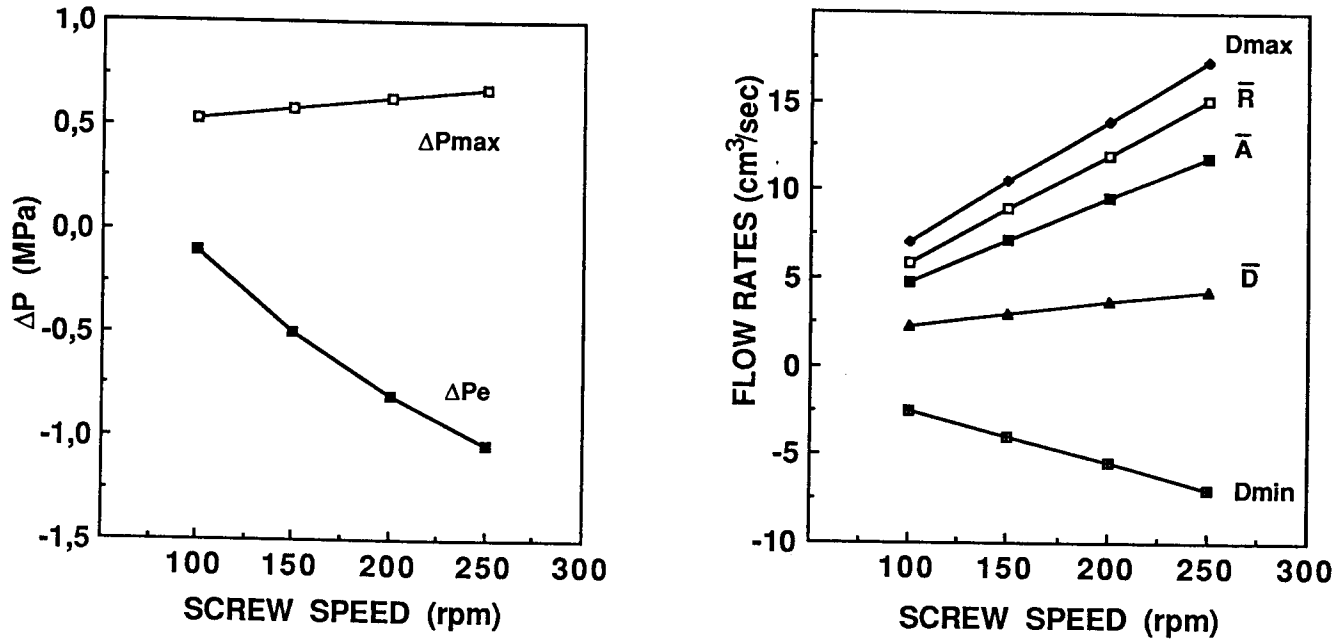

Fig. 7—Influence of screw speed on computed pressure drops and flow rates (feed rate = 30 kg/hr). ΔPmax: pressure drop between the maximum pressure in the RSE and the pressure at the die:ΔPe: pressure drop between the pressure at the entrance of the RSE and the pressure at the die; Dmax and Dmin: maximum and mimimum D-type (Fig. 2) flow rates: R̄, Ā, D̄: average R-type, A-type and D-type flow rates.

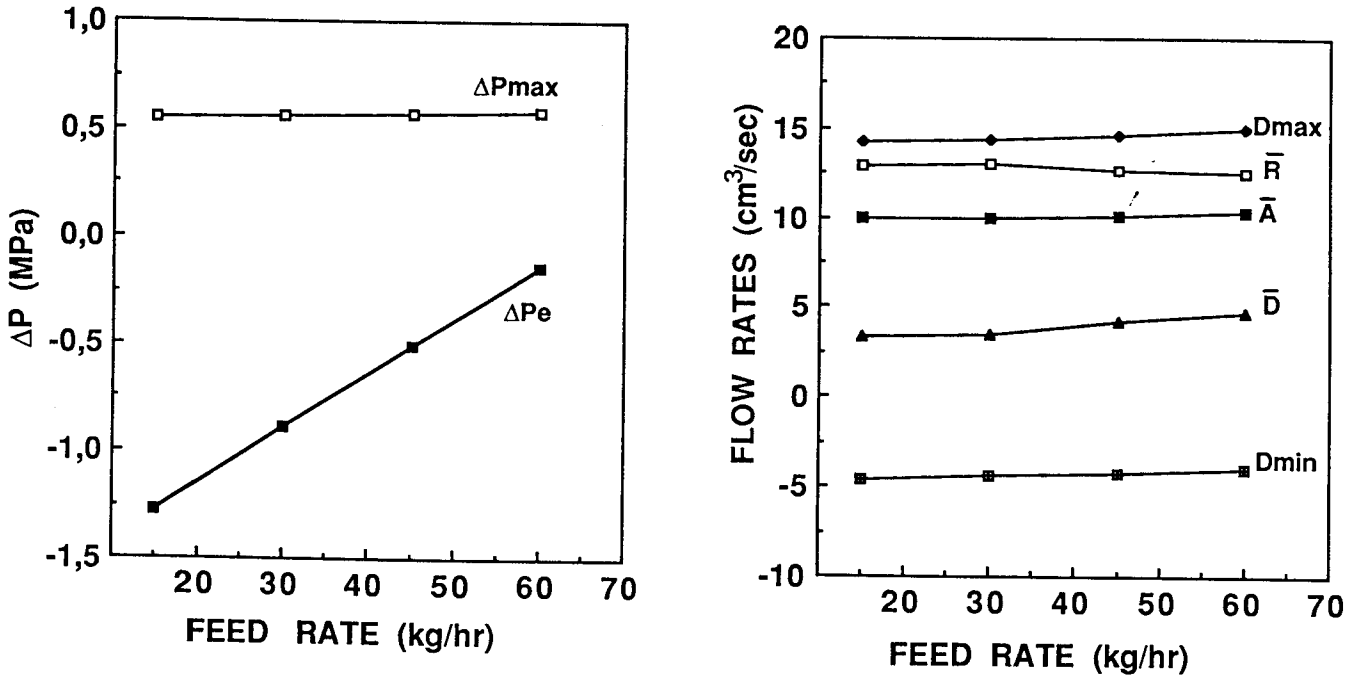

Fig. 8—Influence of feed rate on computed pressure drops and flow rates (screw speed = 200 rpm). ΔPmax, ΔPe, Dmax, Dmin, R̄, Ā, D̄: see Fig. 7.

imately by 10 cm³/sec when screw speed increased from 100 to 250 rpm, but a closer analysis showed that their repartition in each kind of channel remained similar.

The influence of the axial slots width is shown in Fig. 9. ΔPmax and ΔPe increased sharply (+3.0 MPa) when axial slots width decreased (15 to 3 mm). The R and A-type flow rates varied smoothly, the first one increasing (+2 cm³/sec) and the second one decreasing (-2 cm³/sec) with axial slots width (3 to 15 mm); the average value of the D-type flow rate did not change much but it was an artifact of averaging the values, as Dmin and Dmax varied a lot (12–15 cm³/sec) in opposite directions. A closer analysis showed that even the repartition of flow was modified (Fig. 10) when the axial slots width was changed; the pressure field map (Fig. 11) demonstrated that the narrower were the axial slots, the lesser was the dependency of the pressure in a backwarding channel on the pressures in the neighboring channels.

Computed residence time distribution

The knowledge of the flow distribution through the RSE allowed computation of the residence time distribution (RTD) in this part of the screw. The method consisted in simulating the flow of a tracer injected at the entrance. At each step of

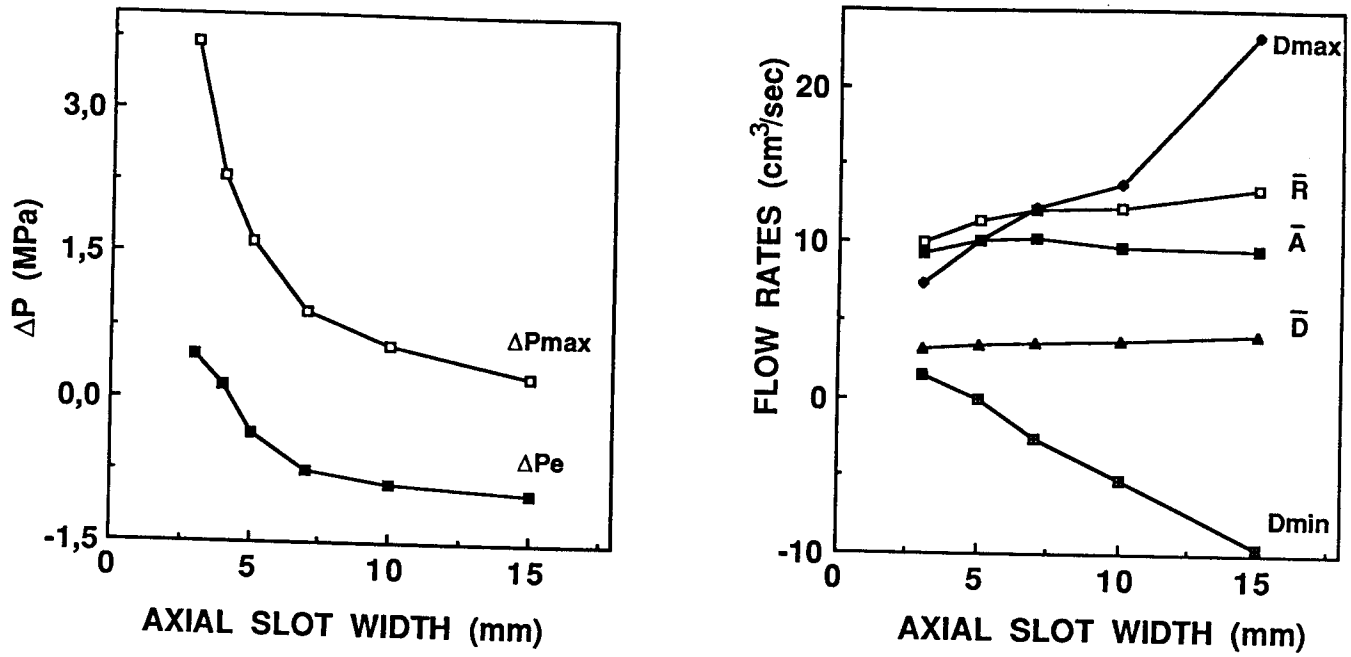

Fig. 9—Influence of axial slots width on computed pressure drops and flow rates (feed rate = 30 kg/hr; screw speed = 200 rpm). ΔPe, dmax, Dmin, R̄, Ā, D̄: see fig.7.

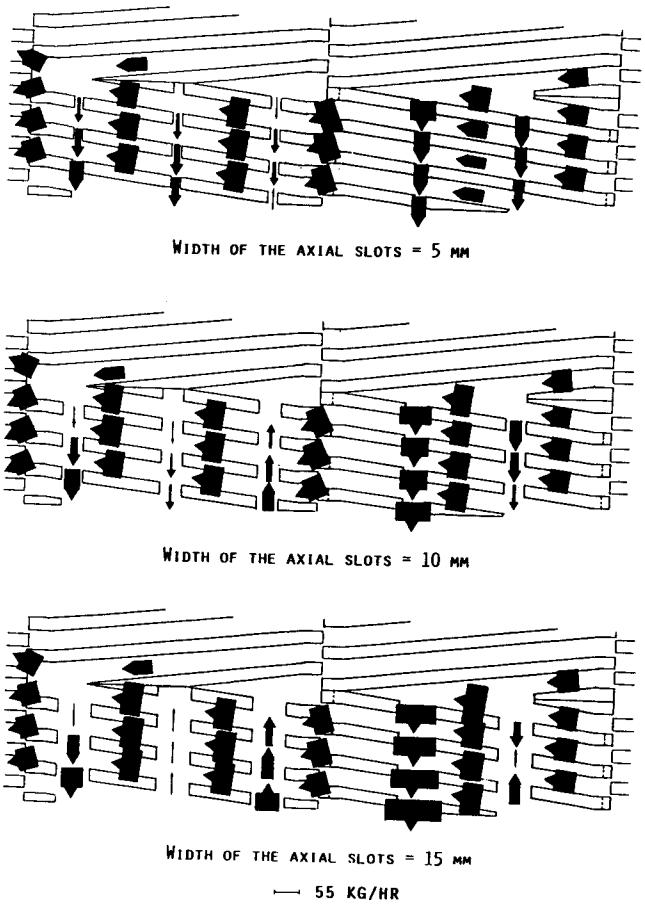

Fig. 10—Computed flow rate distribution in the RSE*: the width of the arrow is proportional to the local flow rate.*

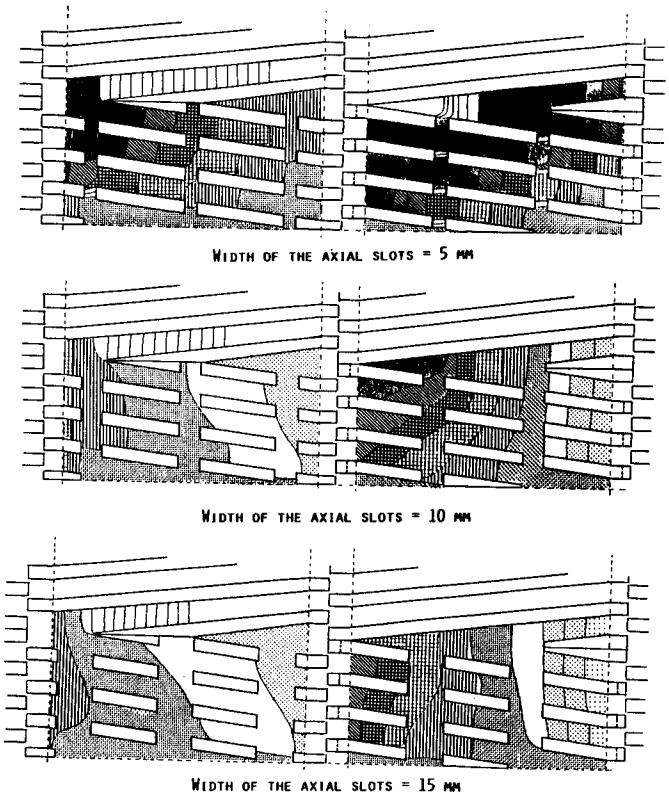

Fig. 11—Computed pressure distribution in the RSE *(each colored zone is 10* MPa *wide from* ▦ *= 4.6* MPa *to* ■ *peq 6.0* MPa*).*

time, the repartition of the tracer was computed according to the different flow paths. For instance, the preceding computations showed that, in the standard conditions, from 100 particles arriving at node (3,4) (Fig. 2), 49 particles went to node (3,3) where they arrived after 0.59 sec and 51 particles went to node (4,4) where they arrived after 0.06 sec; from these 51 particles, 21 went to node (4,3) and 30 to node (5,4).

The residence time distribution was computed by summing the particles arriving at the die during a given amount of time.

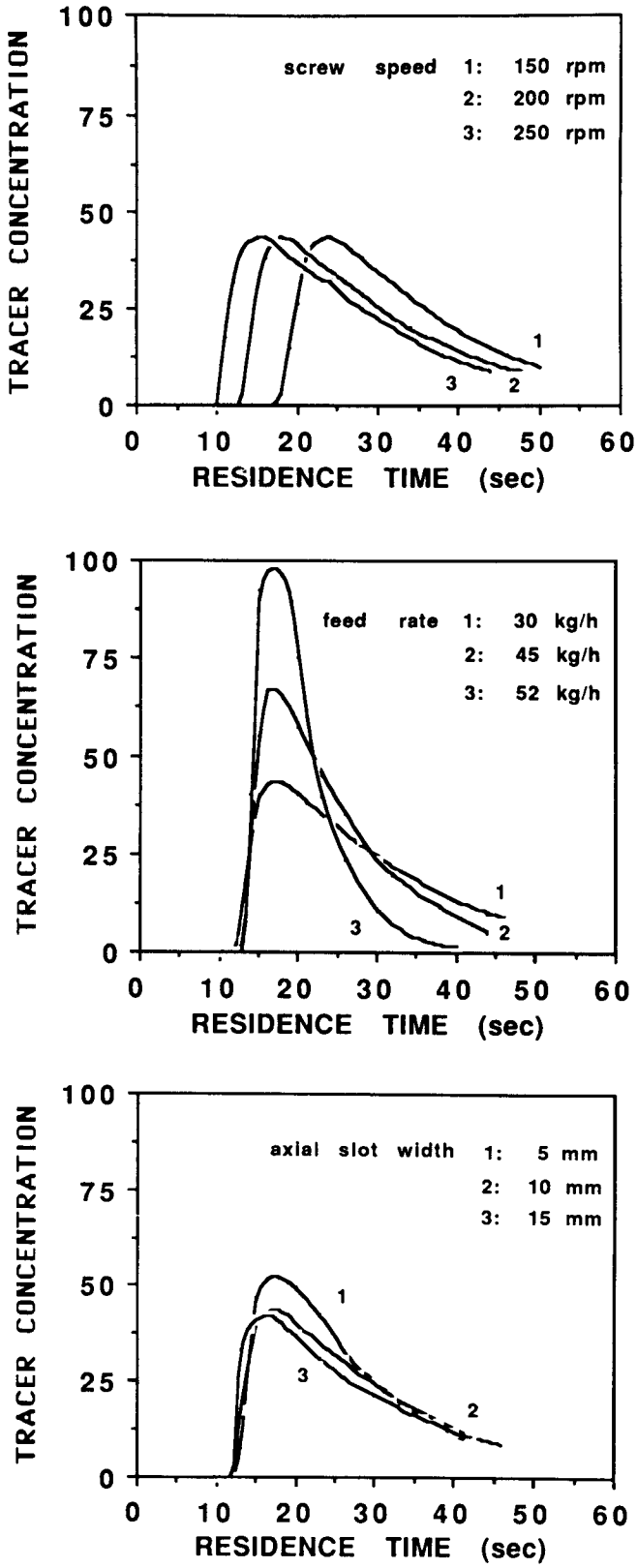

Fig. 12—Computed residence time distribution for different screw speeds, feed rates and axial slots widths.

In the first part of the extruder the residence time was estimated by a plug flow from the models for transport and pressure built up zone (Tayeb, 1986); this assumption is based on the RTD measurements reported by Olkku et al. (1980) where they have the broadening of the RTD curves to the reverse screw element.

The resulting residence time distributions are drawn in Fig. 12 for various screw speed, feed rate and axial slots width. The main conclusions were that the broadening of the distribution decreased strongly when feed rate increased, whereas it did not change considerably with screw speed; on the other hand, the minimum residence time increased mainly when screw speed decreased. The broadening of the distribution decreased when axial slot width decreased (the curve of Fig. 12 being normalized, the higher a curve is, the narrower it is), but this variable and lesser bearing than feed rate in the range tested.

DISCUSSION AND COMPARISON WITH EXPERIMENTAL RESULTS

THE ASSUMPTIONS of Newtonian behavior, isothermicity and quasi-steady geometry were too restrictive to hope for perfect agreement between computed results and experimental data. Therefore, a general comparison with previously published results was undertaken rather than a detailed study. The aim was to determine if the description of flow was correct enough to be included in a global model of the extruder based on these assumptions.

Pressure drop through the reverse screw element

A larger pressure drop is generally thought to be necessary for the product to flow through the RSE, but our results showed that the maximum pressure was only about 0.5–1.0 MPa more than the die pressure. In fact, no experimental verification of a high pressure drop through the RSE has ever been published; moreover, our experimental studies (Della Valle et al., 1987) tend to prove that the pressure drop through the RSE is in the range predicted by the model (about 0.5 MPa). Apart from the influence of axial slots width, the maximum pressure did not vary greatly with the tested parameters.

The evolution of computed pressure with screw speed, total feed rate and axial slot width indicated that it was easier for the material to flow through the RSE at high screw speed, low feed rate or with large axial slot width, which may be observed experimentally.

The difference between the entrance pressure and the die pressure included not only the pressure drop through the RSE but also the increase of pressure generated at the end of the direct screw element and in the transition zone between these two screw elements (Fig. 2: node (0,2) to node (1,4)). So the computed entrance pressure is often lower than the die pressure; this phenomenon may not be observed experimentally, as screw rotation averages experimental pressure between entrance pressure and maximum pressure.

Flow rate field in the reverse screw element

This theoretical study led to several generalized results. The local flow rates in the RSE were quite important compared with the total flow rate going through this element (two to three times larger), due to the existence of large secondary flows; when experimental conditions varied, the flow rates repartition varied only slightly, even if their amplitude might change, particularly with screw speed modifications; when the axial slots width was modified, its main effect concerned the D-type flow rate (going directly through the axial slot).

It was very difficult to imagine an experimental verification of such results, as it seemed difficult to visualize the flow in a real RSE. However, an indirect proof of a good prediction of the flow rate repartition was obtained from the residence time distribution, which was closely linked with the flow rate field. On this topic, experimental observations on the same kind of extruder and with identical screw configuration (Mosso et al., 1982) confirm the computed values in a qualitative man-

ner. Mosso et al. (1982) observed that the broadening of the distribution increases (from 20 to 40 sec) when feed rate decreases (from 9.2 to 6.5 cm^3/sec = 50 to 35 kg/hr) and that the minimum residence time increases (from 35 to 55 sec) mainly when screw speed decreases from (98 to 38 rpm). In our knowledge, nothing has been published on the effect of the axial slot width on the residence time distribution.

If one admits that the broadening of the residence time distribution curve is correlated with the mixing, it can be approximately predicted that mixing in the RSE increases primarily at low feed rate and, to a smaller extent, with large axial slots but is quite independent from screw speed.

SUMMARY AND CONCLUSIONS

THE COMPUTATION METHOD developed in this study was based on the solution of Stokes equation and on writing flow rate conservation in each part of the reverse screw element. It has allowed for the first time, as far as we know, the description of flow of a molten material in this screw element. In spite of the assumed hypotheses (isothermicity, Newtonian flow in each portion of the RSE, quasi-steady geometry), predicted values of pressure drop and residence time distribution were in good agreement with the experimental results.

This study resulted in a relationship between feed rate and pressure drop in the reverse screw element, which is necessary to develop a general model of a twin screw extruder including such a screw element. Moreover, the knowledge of shear rate (which may be computed from Eq. (5) and (6)) and residence time distribution is useful for predicting product transformation from the computation of the energy provided to the product.

NOMENCLATURE

Bs	screw pitch
Cl	distance between screw shafts
Fe	flight width at the top of the channel
Fi	flight width at the bottom of the channel
Fp	shape factor for the pressure flow
Fp_v	shape factor for the pressure flow in the regular channel
Fp_w	shape factor for the pressure flow in the axial slots
Fp_i	shape factor for the pressure flow in the intermeshing zone
Fd	shape factor for the drag flow
Fd_v	shape factor for the drag flow in the regular channel
Fd_w	shape factor for the drag flow in the axial slot
Fd_i	shape factor for the drag flow in the intermeshing zone
h	channel depth
K	consistency
la	axial slots width
lv	channel width
li	channel width in the intermeshing zone
lw	channel length
m	pseudoplasticity index
Na	number of axial slots per turn of screw
P	pressure
P(i,j)	pressure at node i j
ΔPe	pressure drop between the pressure at the entrance of the RSE and the pressure at the die
ΔPmax	pressure drop between the maximum pressure in the RSE and the pressure at the die
$\Delta P/\Delta\theta$	down-channel pressure gradient
$\Delta P/\Delta z$	cross-channel pressure gradient
Qv	down-channel flow rate
Qw	cross-channel flow rate
Qr	flow rate through the regular channel (RSE)
Qd	flow rate through the axial slots (RSE)
Qa	flow rate through the intermeshing zone (RSE)
Re	external screw radius
Ri	internal screw radius
r,θ,z	cylindrical coordinate system
u,v,w	velocity components
Ve,We	velocity components at the barrel
η	Newtonian viscosity
η_v	Newtonian viscosity in the regular channel (RSE)
η_w	Newtonian viscosity in the axial slots (RSE)
η_i	Newtonian viscosity in the intermeshing zone (RSE)
Ψ	intermeshing angle (Fig. 3)
φ	screw pitch angle
Ω	screw rotation speed

REFERENCES

Booy, M.L. 1978. Geometry of fully wiped twin-screw equipment. Polym. Eng. Sci. 18 (12):973.

Booy, M.L. 1980. Isothermal flow of viscous liquids in corotating twin screw devices. Polym. Eng. Sci. 20 (18):1220.

Bruin, S., Van Zuilichem, D.J., and Stolp, W. 1978. A review of fundamental and engineering aspects of extrusion of biolpolymers in a single screw extruder. J. Food Proc. Eng. 2:1.

Colonna, P., Melcion, J.P., Vergnes, B., and Mercier, C. 1983. Flow, mixing and residence time distribution of maize starch within a twin-screw extruder with a longitudinally-split barrel. J. cereal Sci. 1:115

Della Valle, G., Tayeb, J., and Melcion, J.P. 1987. Relationship between extrusion variables and pressure and temperature during twin-screw extrusion cooking of starch. J. Food Eng. In press.

Denson, C.D. and Hwang, B.K. 1980. The influence of the axial pressure gradient on flow rate for newtonian liquids in a self wiping, co-rotating twin screw extruder. Polym. Eng. Sci. 20 (14):965.

Fletcher, S.I., Mac Master, T.J., Richmond, P., and Smith, A.C. 1984. Physical and rheological assesment of extrusion cooked maize. In "Thermal Processing and Quality of Food," P. Zeuthen et al. (Ed.), p. 223. Elsevier, London.

Harmann, D.V. and Harper, J.M. 1974. Modeling a forming food extruder. J. Food Sci. 39:1099

Harper, J.M. 1981. "Extrusion of Food," Vol. 1 and 2. CRC Press, Boca Raton, FL.

Janssen, L.P.B.M. 1978. "Twin Screw Extrusion." Elsevier, Amsterdam.

Linko, P., Colonna, P., and Mercier, C. 1981. High temperature short-time extrusion-cooking. Cereal Sci. Technol., Vol. 4, p. 145. Am. Assoc. Cereal Chem., St Louis, MN.

Martelli, F.G. 1983. "Twin-screw Extruders: a Basic Understanding." Van Nostrand Reinhold Company, New York.

Masheri, J..C. and Wyman, C.E. 1980. Mixing in an intermeshing twin-screw extruder chamber: combined cross and down channel flow. Polym. Eng. Sci. 20 (9):601.

Mosso, K., Jeunik, J., and Cheftel, J.C. 1982. Temperature, pression et temps de sejour d'un melange alimentaire dans un cuiseur-extrudeur bivis: influence des parametres operatoires. Ind. Agric. Alim. 99 (1–2):5.

Olkku, J., Antila, J., Heikkinen, J., and Linko, JP. 1980. Residence time distribution in a twin screw extruder. In "Food Process Engineering," Vol. 1, P. Linko et al. (Ed.),p. 791. Applied Science Publisher, London.

Pisipati, R. and Fricke, A.L. 1980, Computer simulation of a single screw extruder. In "Food Process Engineering," Vol. 1, P. Linko et al. (Ed.), p757. Applied Science Publishers, London.

Rauwendaal, C. 1986. "Polymer Extrusion." Mauser Verlag, Munich.

Tayeb, J. 1986. Approche théorique et expérimentale de la cuisson-extrusion de l'amidon. Doctorat thesis, Ecole des Mines De Paris, Paris.

Vergnes, B., Villemaire, J.P., Colonna, P., and Tayeb, J. 1985. Etude du comportement de l'amidon en phase fondue à l'aide d'un rhéomètre à pre-cisaillement: le Rhéoplast. Cahier du Gr. Franc. Rhéol. In press.

Vergnes, B. and Villemaire, J.P. 1987. Rheological behavior of low moisture molten maize starch. Rheol. Acta (submitted for publication).

Vergnes, B., Villemaire, J.P., Colonna, P., and Tayeb, J. 1987. Interrelationships between thermomechanical treatment and macromolecular degradation of maize starch in a novel rheoimeter with preshearing. J. Cereal Sci. 5 (1): 189.

Wyman, C.E. 1975. Theoretical model for intermeshing twin screw extruders; axial velocity profile for shallow channels. Polym. Eng. Sci. 15 (8): 606.

Yacu, W.A. 1985. Modelling a twin-screw co-rotating extruder. J. Food Eng. 8 (1): 1.

Ms received 3/2/87; revised 9/5/87; accepted 9/9/87.

The authors thank Dr. J.F. Agassant (CEMEF-Sophia Antipolis) for helpful discussions.

APPENDIX

Expression of coefficients A, B, C, D, E, F

The coefficients A, B, C, D, E, F in Eq. (9) to (11) may be obtained by identification from Eq. (7) and (8)

Expression of A and B (R-type flow rate):

$$A = Fd_v\, lv \frac{\Omega\, Re^2 \cos\varphi}{2}\left[1 - \left(\frac{Ri^2}{Re^2 - Ri^2} \ln\left(\frac{Re}{Ri}\right)^2\right)\right]$$

$$B = -\, Fp_v\, lv \frac{Na}{16\,\eta_v\,\pi}(Re^2 - Ri^2)\left[1 - \left(\frac{2\,Re\,Ri}{Re^2 - Ri^2} \ln\left(\frac{Re}{Ri}\right)\right)^2\right]$$

Expression of C and D (D-type flow rate):

$$C = Fd_w\, lw\, \Omega\, Re^2 \sin\varphi \left[1 - \left(\frac{1 - \frac{Ri}{Re}}{\ln\left(\frac{Re}{Ri}\right)}\right]\right.$$

$$D = -\, Fp_w\, lw \frac{1}{2\,\eta_w\,(Fe + Fi)}\left[\frac{2}{3}(Re^3 - Ri^3) - \left(\frac{Re^3 - Ri^3 - Ri\,Re^2 + Ri^2\,Re}{\ln\left(\frac{Re}{Ri}\right)}\right)\right]$$

Expression of E and F (A-type flow rate):

The expression of E and F must take into account the fact that A-type flow rate is going through regular backwarding channel and through the intermeshing zone, these two parts being geometrically related by the relative screw position ($\pi - 2\,\Psi$ factor in F).

$$E = \frac{\left[Fd_v\, lv \frac{\Omega\, Re^2 \cos\varphi}{2}\right]\left[Fp_i\, li \frac{h^2}{8\,\eta_i}\right]\left[1 - \left(\frac{Ri^2}{Re^2 - Ri^2} \ln\left(\frac{Re}{Ri}\right)^2\right)\right]}{\left[Fp_v\, lv \frac{Re^2 - Ri^2}{8\,\eta_v}\right]\left[1 - \left(\frac{2\,Re\,Ri}{Re^2 - Ri^2} \ln\left(\frac{Re}{Ri}\right)\right)^2\right] + \left[Fp_i\, li \frac{h^2}{8\,\eta_i}\right]}$$

$$F = \frac{-\left[Fp_v\, lv \frac{Re^2 - Ri^2}{8\,\eta_v}\right]\left[Fp_i\, li \frac{h^2}{8\,\eta_i}\right]\left[1 - \left(\frac{2\,Re\,Ri}{Re^2 - Ri^2} \ln\left(\frac{Re}{Ri}\right)\right)^2\right]}{\{\pi - 2\,\Psi\}\left\{\left[Fp_v\, lv \frac{Re^2 - Ri^2}{8\,\eta_v}\right]\left[1 - \left(\frac{2\,Re\,Ri}{Re^2 - Ri^2} \ln\left(\frac{Re}{Ri}\right)\right)^2\right] + \left[Fp_i\, li \frac{h^2}{8\,\eta_i}\right]\right\}}$$